Proceedings of the 20th International Conference on Soil Mechanics and Geotechnical Engineering– Rahman and Jaksa (Eds)

Cyclic lateral pipe-soil interaction in clayey soils under constant vertical force

Interaction cyclique latérale tuyau-sol dans les sols argileux sous une force verticale constante

Marcio S. S. Almeida, José R. M. S. Oliveira & Maria C. F. Almeida
Federal University of Rio de Janeiro, Rio de Janeiro, Rio de Janeiro, Brazil, marciossal@gmail.com

Juliana Pessin
Department of Geotechnical Engineering, University of São Paulo at São Carlos, formerly at Graduate School of Engineering COPPE, Federal University of Rio de Janeiro, São Carlos, São Paulo, Brazil

Pablo C. Trejo
College of Civil Engineering, National University of Engineering, formerly at Graduate School of Engineering COPPE, Federal University of Rio de Janeiro, Lima, Peru

Fernando Saboya Jr.
Department of Civil Engineering, State University of Norte Fluminense Darcy Ribeiro, Campos dos Goytacazes, Rio de Janeiro, Brazil

ABSTRACT: This work intends to contribute to the current state of knowledge on the mechanisms of cyclic lateral pipe-soil interaction in the seabed by means of centrifuge modeling. In that way, a vertical load-controlled system provided the simulation of pipe weight during the lateral movement. Four lateral tests reproduced pipe prototypes of 0.5 m in diameter, cycling on a kaolin clay seabed. Two undrained strength profiles were prepared and characterized by T-bar tests prior to the cyclic actuation. As a response to the controlled vertical force system, the embedment ranged from 10% to 80% of the pipe diameter, depending on the strength profile. In order to consider the shallow embedment reached in the first sweep, the undrained strength was adjusted considering T-bar factor changes. Cyclic lateral responses indicated a light-pipe on a normally-penetrated behavior. Experimental responses of embedment and lateral resistances (breakout and berm ones) were compared with analytical models available in the literature. Cyclic berm resistance was strictly related to the vertical force, emphasizing the importance of vertical force to predict large deformation resistance, even for greater embedment values.

RÉSUMÉ : Ces travaux visent à contribuer à l'état actuel des connaissances sur les mécanismes de l'interaction cyclique latérale tuyau-sol dans le fond marin au moyen de la modélisation par centrifugation. De cette façon, un système vertical contrôlé par la charge a permis de simuler le poids du tuyau pendant le mouvement latéral. Quatre essais latéraux ont reproduit des prototypes de conduites de 0,5 m de diamètre, circulant sur un fond marin d'argile kaolinique. Deux profils de résistance non drainés ont été préparés et caractérisés par des tests de barre en T avant l'actionnement cyclique. En réponse au système de force verticale contrôlée, l'enrobage variait de 10% à 80% du diamètre du tuyau, en fonction du profil de résistance. Afin de tenir compte de l'enfoncement peu profond atteint lors du premier balayage, la résistance non drainée a été ajustée en tenant compte des changements de facteur de barre en T. Les réponses latérales cycliques indiquaient un conduit de lumière sur un comportement normalement pénétré. Les réponses expérimentales de l'enfoncement et des résistances latérales (cassure et berme) ont été comparées aux modèles analytiques disponibles dans la littérature. La résistance cyclique des talus était strictement liée à la force verticale, soulignant l'importance de la force verticale pour prédire une grande résistance à la déformation, même pour des valeurs d'enfoncement plus élevées.

KEYWORDS: Pipelines; clay; cyclic interaction; lateral movement; soil interaction.

1 INTRODUCTION

The evaluation of lateral soil-pipe forces during large loading cycles is fundamental in pipeline design. Many authors (Cheuk et al. 2007, Dingle et al. 2008, Merifield et al. 2009, Cheuk & White 2010, Oliveira et al. 2010, Lee et al. 2011, Chatterjee et al. 2012, Rismanchian et al. 2019, Kong et al. 2020 and Trejo et al. 2020) have made contributions towards the understanding of soil-pipe interaction mechanisms on offshore pipelines.

Pipeline behavior is affected by horizontal movements (Morris & Webb 1988; Wang et al. 2017; White et al. 2017), which form a trench in the soil as the pipe displaces laterally. These cyclic movements result in pipe-soil interaction at the trench wall, also called berm, and can result in lateral and vertical forces increase on the pipe. Therefore, a significant lateral resistance of the soil is mobilized when the pipe is in contact with the soil berm (You et al. 2008; Rismanchian et al. 2019). Soil berms restrict the increase in lateral displacements in situations of high compression stresses along the pipe structure (Bruton et al. 2006), such as pipe buckling which is caused by the combination of temperature increase and axial restraints on the pipe.

Lateral resistance is associated with forces at breakout (peak) and after breakout. The breakout resistance can also be calculated as the sum of a friction and a passive components, while the force after breakout is basically associated with the increase in lateral resistance due to the formation and augmentation of a soil berm in front of the pipe, as it moves.

2 MATERIALS AND METHODS

A series of four lateral cyclic interaction tests were performed on artificial kaolin clay, which is a widely used material in centrifuge modeling (Dingle et al. 2008). The tests were performed in a mini geotechnical beam centrifuge (Almeida et al. 2014), equipped with a bidirectional actuator and a load-controlled vertical system able to simulate pipe weight.

2.1 *Soil sample*

The kaolin clay was mixed with water and formed a slurry with a moisture content of 81% (1,5 times the liquid limit). The sample was consolidated in-flight at 100*g* using surcharges of 120 kPa and 20 kPa, defining profiles P1 and P2, respectively. The surcharge was removed before the start of the lateral interaction test. The submerged unit weight of the consolidated clay was 6.4 kN/m³. T-bar tests were carried out to provide the undrained shear strength (S_u) profiles of the samples and to check the repeatability of the profiles, shown in Figure 1. The legend in the graph indicates the respective lateral test for each sample. The first number indicates the soil profile (P1 or P2), and the second the repeatability of the tests (two tests performed for each condition).

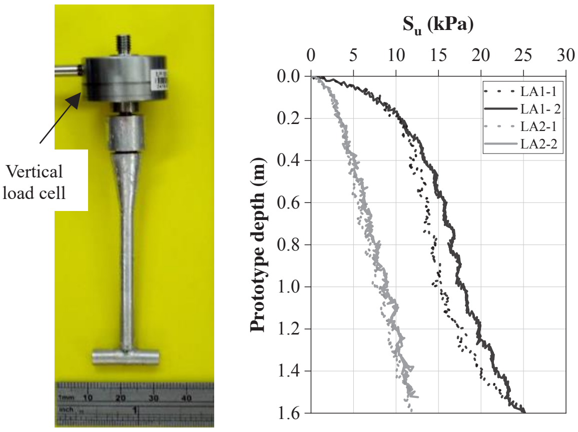

(a) (b)

Figure 1. Undrained shear resistance: (a) T-bar instrument and (b) undrained shear resistance profiles.

2.2 *Lateral cyclic interaction tests*

The lateral interaction tests were performed with a model-prototype ratio of 1:33 (N = 33). They took into account cyclic interaction and simulated a constant displacement of 3 pipe diameters over 12 cycles. A lateral pipe model of 15 mm was used to simulate a pipe diameter of 0.5 m in the prototype scale. It was instrumented by a vertical and a flexural load cell to record vertical force (and to feed the vertical load system) and lateral resistance, respectively, as shown in Figure 2.

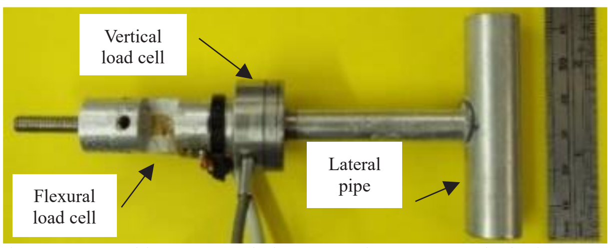

Figure 2. Lateral instrumented pipe (rotated 90° counterclockwise).

Table 1 summarizes the characteristics of the lateral interaction tests. All lateral tests, *LA1-1*, *LA1-2*, *LA2-1*, *LA2-2*, were performed under the same pipe weight differing only by the soil strength profile.

Table 1. Centrifuge model test parameters (model scale).

Characteristics	*Value*	*Unit*
Pipe diameter (D)	15	mm
Pipe length (4D)	60	mm
Range of movement (3D)	45	mm
Cycles	12	-
Pipe weight (V)	2	N
Actuation speed (undrained)	0,86	mm/s
Clay layer thickness	70	mm
Water layer thickness on clay	20	mm
Centrifuge acceleration	33	*g*

3 RESULTS AND DISCUSSIONS

3.1 *Pipe embedment (w)*

During lateral interaction tests, the initial pipe embedment was a response to pipe weight imposition. However, once the cyclic interaction started, the embedment increased due to the lateral movement and as a response to the pipe weight. The typical embedment response indicated a trench formation centered in the middle of the sweep, as shown in Figure 3, where *u* is the lateral displacement.

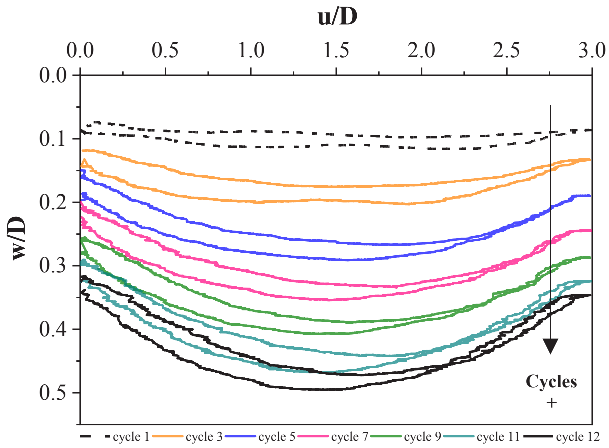

Figure 3. Typical embedment response during lateral interaction (LA1-2).

The pipe embedment of tests performed in P1 ranged from 10% to 50% (Figure 3), while in profile P2 ranged from 10 to 80%, on average. It means that the softer soil provided an embedment 60% higher after lateral cyclic interaction. In addition, it has been noted that the embedment tends to stabilize in the last cycles.

3.2 *Lateral resistance (H)*

The typical cyclic lateral interaction response achieved in profiles P1 and P2 are presented in Figures 4a and 4b, respectively. Only odd cycles and the cycle 12 were presented to facilitate visualization.

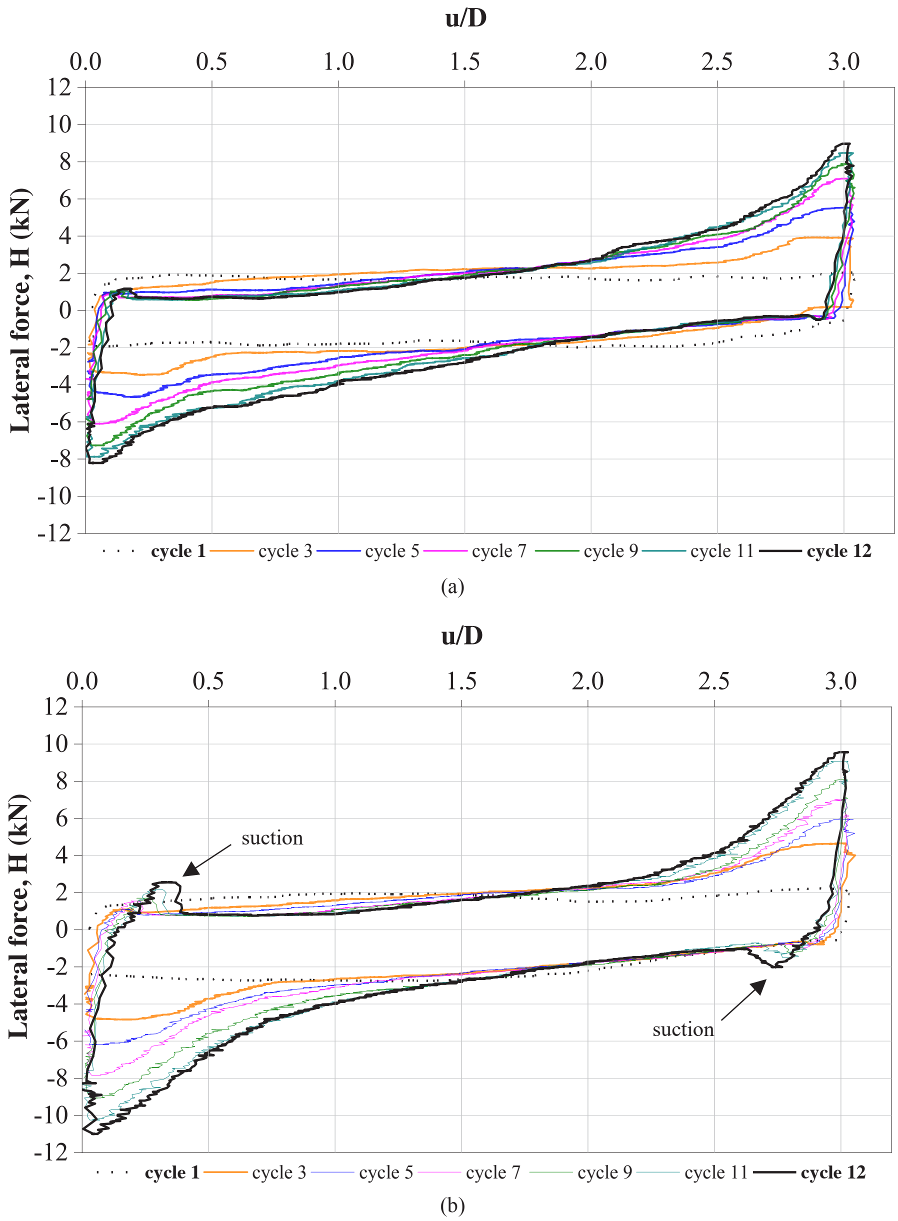

Figure 4. Typical lateral resistance response during lateral interaction for (a) P1 and (b) P2.

The magnitude of the lateral force achieved in both profiles is similar. However, the suction developed in the ends of the sweeps, i.e., the moment the pipe leaves the berm, is more pronounced in the softer clay (P2), especially in the last cycles. This behavior might be related to pipe embedment increase in the last cycles, which also increases the amount of soil behind the pipe and therefore improve suction conditions.

The following items present predictions and results of the lateral breakout and berm resistances. Except cyclic resistance, breakout and berm resistance are reached in the first sweep, where the embedment found is close to 10% of pipe diameter. In such a low embedment, it is believed that the failure envelopes are not completely formed yet. Therefore, the undrained resistance S_u used in the analyses of lateral resistance for P1 and P2 was determined according to the proposition of Barboza-Cruz e Randolph (2007), expressed in Eq. 1:

$$S_u(kPa) = 5 + 1.5(w/D) \quad (1)$$

3.2.1 *Breakout resistance (H_{brk})*

Breakout resistance has been considered as the sum of the frictional resistance H_f and the passive component H_p required to lift and deform the region of soil in front of the pipe (Verley & Lund 1995, Bruton et al. 2006 and Dendani & Jaeck 2007), according to Eqs. 2-4:

$$H_{brk} = H_f + H_p \quad (2)$$

$$H_f = \mu V \quad (3)$$

$$H_p = S_u . D . a \left(\frac{S_u}{\gamma' D}\right)^b \left(\frac{w}{D}\right)^c \quad (4)$$

where μ is the friction factor, S_u is the undrained strength obtained according to Eq. 1, respective to the average embedment in the first cycle and γ' is the submerged weight of the soil. Each author proposed different constants *a*, *b*, and *c* to be used in Eq. 4 to adjust their data, as shown in Table 2.

Table 2. Parameters used for assessing breakout resistance according to different authors.

Coefficient	*Verley & Lund (1995)*	*Bruton et al. (2006)*	*Dendani & Jaeck (2007)*
a	4.130	3.000	2.300
b	-0.392	-0.500	0.000
c	1.310	1.000	1.000
μ	0.200	0.200	0.200

White et al. (2017) presented a different approach to evaluate the breakout resistance, based on laboratory tests of undrained lateral pipe-soil behavior, according to Eq. 5:

$$\frac{H_{brk}}{S_u D} = 0.61\left(\frac{w}{D}\right)^{1.7} + 0.23\left(\frac{V\prime}{S_u \cdot D}\right)^{0.83} + 0.6\left(\frac{\gamma\prime \cdot D}{S_u}\right)\left(\frac{w}{D}\right)^{2} \quad (5)$$

Oliveira et al. (2010) proposed Eq. 6 to estimate the lateral breakout resistance. The constant n is associated with the development of failure surfaces, which represents the amount of mobilized resistance during breakout.

$$\frac{H_{brk}}{S_u D} = 5\ atan\left(\frac{n.w}{D}\right) \quad (6)$$

The breakout resistance found in this study was compared with the predictions presented in this section and with sideswipe tests performed by Trejo (2015), which considered a broader range of pipe embedments but used similar soil profiles to this work. The result is shown in Figure 5, indicating a reasonable agreement.

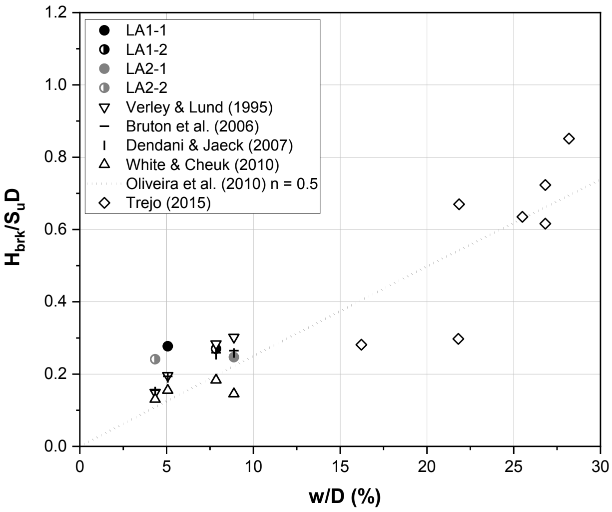

Figure 5. Breakout resistance.

3.2.2 *Berm resistance (H_{berm})*

White & Cheuk (2008) proposed Eq. 7 to evaluate the berm resistance based on a tri-linear model of lateral interaction.

$$\frac{H_{berm}}{S_u D} = \left(\propto_0 \lambda \left(\frac{V}{S_u D}\right)^{\beta} . \frac{u}{D}\right)^{\delta} \quad (7)$$

where α_0 and β are parameters that relate the applied vertical load and pipe embedment, λ and δ relate the size and berm resistance, and u is the lateral displacement.

The results of the present work, compared with White & Cheuk (2008), show some scattering indicating that the behavior could not be properly predicted, as indicated in Figure 6.

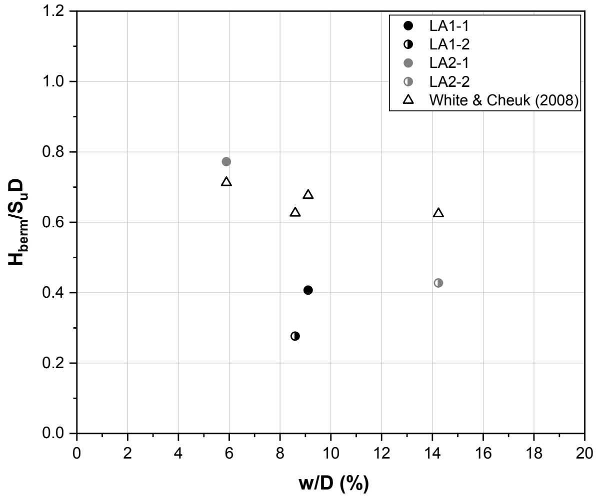

Figure 6. Berm resistance.

3.2.3 *Cyclic berm resistance*

Under pipe weight, during lateral cyclic pipe-soil interaction, a berm is formed in the extremes of sweeps, the pipe embedment increases gradually, and more soil is added to the berm as the interaction progresses. The cyclic berm resistance normalized by the respective vertical force is shown in Figure 7, as circle points. The tests performed in softer soil profiles achieved a higher lateral resistance, but this difference appears mainly in the first cycle.

Once the pipe reaches the berm, the lateral berm resistance increases besides the residual resistance (achieved in the first sweep) by an additional resistance ΔH_{berm}. For each sweep, ΔH_{berm} is determined as the difference between the actual lateral resistance and the residual resistance, normalized by the respective vertical force. The average berm resistance found in each cycle is obtained according to Eq. 8:

$$\Delta(H/V)_{berm,n} = (H/V)_{berm,\boldsymbol{n}} - (H/V)_{berm,\mathbf{1}} \quad (8)$$

These results, presented as triangular points in Figure 7, show that the variation of lateral resistance with respect to the first cycle $\Delta(H/V)_{berm}$ varies almost linearly, and it is similar for both profiles. Bruton et al. (2006) reached a $\Delta(H/V)_{berm}$ around 1.5 in 5 cycles, whereas 0.4 was found in the present study.

Although the lateral berm resistance increases with the cyclic interaction, the increment of lateral berm resistance related to the previous cycle, expressed in Eq. 9, is almost constant.

$$\delta(H/V)_{berm} = (H/V)_{berm,\boldsymbol{n}} - (H/V)_{berm,\boldsymbol{n-1}} \quad (9)$$

The increment $\delta(H/V)_{berm}$ was similar for all tests and around 0.075, as if the amount of material dragged was the same in all cycles, even in different soil profiles.

Therefore, the cyclic lateral berm resistance results presented in this section emphasize the importance of the berm resistance achieved in the first sweep to predict the cyclic resistance.

3.3 *Failure envelope approach*

The failure envelope approach provides a consistent calculation method for lateral resistance that does not require a split between frictional resistance and passive resistance. Besides, the envelopes indicate the tendency of pipeline embedment increasing according to the magnitudes of vertical and horizontal forces and the size of the envelope, which depends on the embedment (Randolph & Gourvenec 2011).

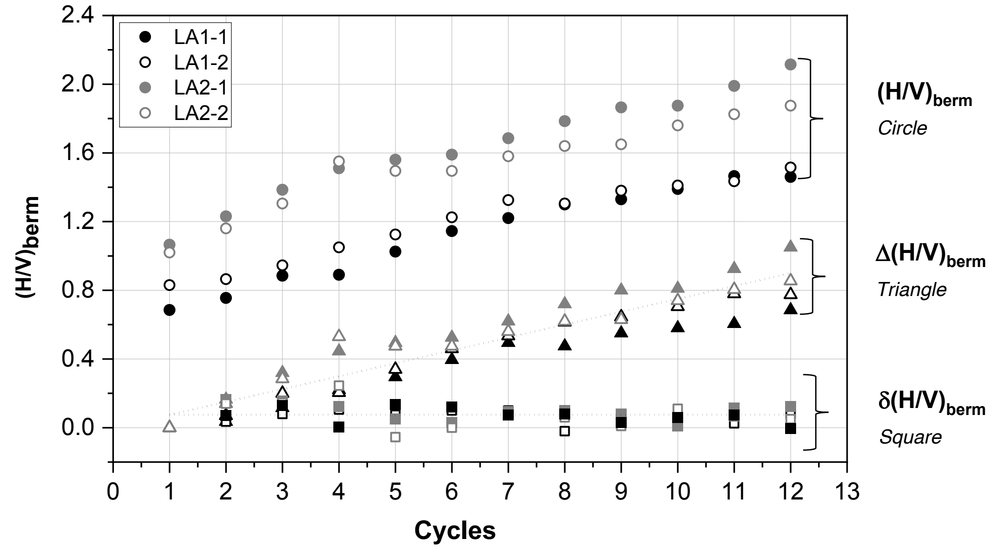

Figure 7. $(H/V)_{berm}$ ratio with cycles.

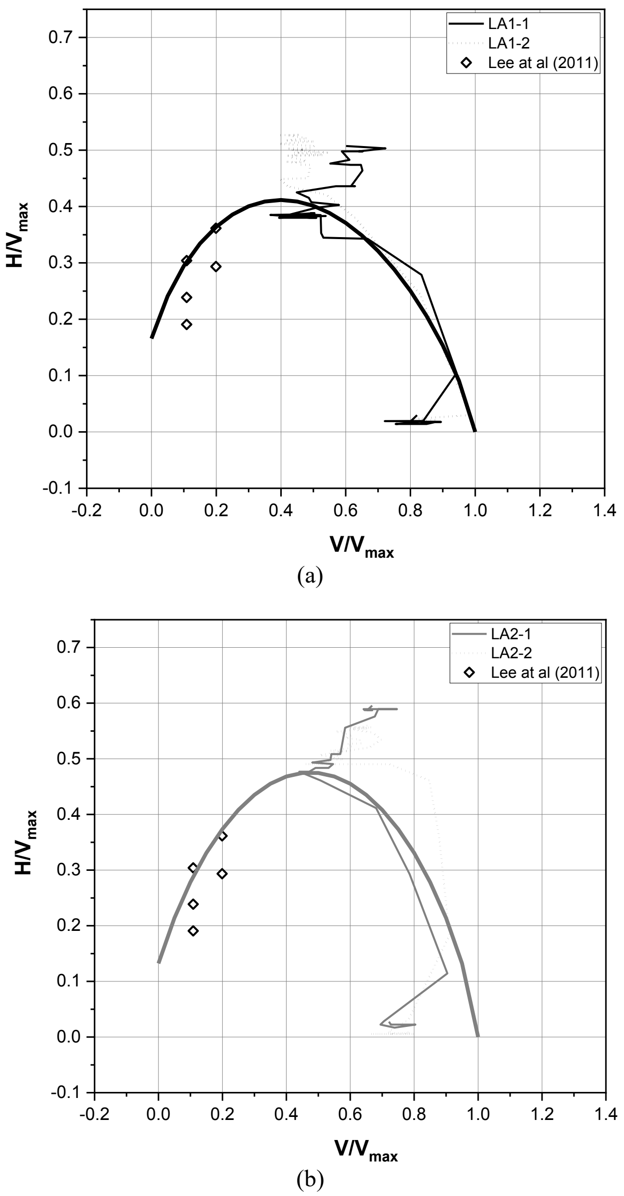

(a)

(b)

Figure 8. Yield surfaces proposed for lateral tests: (a) P1 and (b) P2.

Horizontal resistance relative values for small and large displacements can be estimated through the envelope approach (Randolph & White 2008b, Merifield et al. 2008a,b). In this case, the yield envelope might be generically expressed according to Eq. 10.

$$F = \frac{H}{V_{max}} - \beta_0 \left(\frac{V}{V_{max}} + t\right)^{\beta_1} \left(1 - \frac{V}{V_{max}}\right)^{\beta_2} = 0 \qquad (10)$$

where β_0 is a parameter that relates to β_1 and β_2 (β_1 depends on the friction ratio of pipe-soil interface and the embedment and β_2 only on the embedment). β_1 and β_2 define the peak position of the failure envelope.

Lee et al (2011) conducted two types of lateral breakout tests to investigate the breakout resistance of a partially embedded pipelines: probe and sideswipe tests. During sideswipe tests pipe embedment was constant, and during the probe tests, the vertical load was constant. The yield points of probe tests presented by these authors were plotted along with the results of the present work showing very good agreement. Two yield surfaces were proposed, one for the lateral tests carried out in profile 1 and another for profile 2, as indicated in Figures 8a and 8b, respectively.

4 CONCLUSIONS

This work presented four lateral centrifuge tests simulating pipe prototypes of 0.5 m in diameter, cycling laterally on a kaolin clay seabed in two different undrained strength profiles.

Cyclic lateral responses indicated a light-pipe on a normally-penetrated behavior. The embedment during the tests ranged from 10% to 80% of the pipe diameter as a response to the fixed vertical force value during the lateral cycles.

The pipe embedment increase was found to be related to suction increase, particularly in the last lateral cycles, where the amount of soil behind the pipe migh improve suction generation conditions.

Experimental responses of embedment and lateral resistances (breakout and berm ones) were compared with analytical models available in the literature. Lateral breakout resistance agreed relatively well with predictions from Oliveira et al. (2010).

The berm resistances were compared with predictions from White & Cheuk (2008) but with poorly agreement. Cyclic berm resistance was found to be strictly related to the vertical force, emphasizing the importance of vertical force to predict large deformation resistance, even for greater embedment values.

Envelope analysis was also conducted and the results of this work compared with data from Leet et al (2011) showing good accordance. In general, envelope analysis was found to be the most adequate procedure to predict lateral pipe-soil behavior since takes into account not only the embedment but mostly the acting vertical force, which is directly associated with the lateral mobilization during large displacements.

5 ACKNOWLEDGEMENTS

The authors would like to acknowledge FINEP and TECHNIP for the financial support and the interest in this study. This research was financed in part by the "Coordenação de Aperfeiçoamento de Pessoal de Nível Superior" (CAPES) and by CNPq, Brazilian Research Council.

6 REFERENCES

Barboza-Cruz E.R., and Randolph M.F. 2005. Bearing capacity and large penetration of a cylindrical object at shallow embedment. *Proc. Frontiers in Offshore Geotechnics*, Perth, Australia, 615–621.

Bruton, D. A. S., White, D. J., Cheuk, C., Bolton, M., and Carr, M. 2006. Pipe/soil interaction behavior during lateral buckling, including large-amplitude cyclic displacement tests by the Safebuck JIP. In: *Proceedings of Offshore Technology Conference*, Houston, Texas, pp. 1-10.

Chatterjee S., White D.J. and Randolph M.F. 2012. Numerical simulations of pipe-soil interaction during large lateral movements on clay. *Géotechnique* 62(8), 693-705.

Cheuk C.Y., White D.J. and Bolton M.D. 2007. Large-scale modelling of soil-pipe interaction during large amplitude movements of partially-embedded pipelines. *Canadian Geotechnical Journal*. 44(8), 977-996.

Cheuk, C.Y. and White, D.J. 2010. Modelling the dynamic embedment of seabed pipelines. *Géotechnique*. 61 (1), 39-57.

Dendani, H., and Jaeck, C. 2007. Pipe-soil interaction in highly plastic clays". *International Offshore Site Investigation and Geotechnics Conference*, v. 21, n. 4, pp. 1166–1171.

Dingle H.R.C., White D.J., and Gaudin C. 2008. Mechanisms of pipe embedment and lateral breakout on soft clay. *Canadian Geotechnical Journal*. 45: 636–652.

Kong D., Zhu J., Wu L. and Zhu B. 2020. Break-out resistance of offshore pipelines buried in inclined clayey seabed. *Journal of Applied Ocean Research* 94.

Lee, Y. S., Smith, C. C., and Cheuk, C. Y. 2011. Lateral Breakout Resistance of Shallowly Embedded Offshore Pipelines. *Procedia Engineering*, v. 14, pp. 1690–1695.

Merifield R.S., White D.J. and Randolph M.F. 2009. the effect of surface heave on the response of partially embedded pipelines on clay. *Journal of Geotechnical and Geoenvironmental Engineering*. 135(6), 819–829.

Merifield, R., White, D. J., and Randolph, M. F. 2008b. The effect of pipe-soil interface conditions on undrained breakout resistance of partially-embedded pipelines. *International Conference on Advances in Computer Methodology and Analysis in Geomechanics*, Goa, India.

Merifield, R., White, D. J., Randolph, M. F. 2008a. The ultimate undrained resistance of partially embedded pipelines. *Géotechnique*. 58 (6), 461–470,.

Oliveira J.R.M.S., Almeida M.S.S., Almeida M.C.F., and Borges R.G. 2010. Physical modeling of lateral clay-pipe interaction. *Journal of Geotechnical Geoenvironmental Engineering*.136(7), 950–956.

Randolph, M. F., and White, D. J. 2008. Upper-bound yield envelopes for pipelines at shallow embedment in clay. *Géotechnique*, 58(4), 297–301.

Randolph, M., and Gourvenec, S. 2011. *Offshore Geotechnical Engineering*, 1 ed. Oxon, Spon Press.

Rismanchian A., White D.J., Randolph M.F., and Martin C.M. 2019. Shear strength of soil berm during lateral buckling of subsea pipelines. *Journal of Applied Ocean Research 90*.

Trejo, P. C., Oliveira J.R.M.S., Almeida M.S.S., Almeida M.C.F., and Vignoles, M. A. 2020. A procedure to estimate the lateral force in clay-pipe interaction after breakout. *Revue Française de Géotechnique*, 168, 3.

Verley, R., and Lund, K.M. 1995. A soil resistance model for pipelines placed on clay soils. *Proceedings of International Conference on Offshore Mechanics and Artic Engineering*. American Society of Mechanical Engineers, New York, 225-232.